

Experimental Assessment of Joint Range-Doppler Processing to Address Clutter Modulation from Dynamic Radar Spectrum Sharing

Brandon Ravenscroft¹, Jonathan W. Owen¹, Benjamin H. Kirk², Shannon D. Blunt¹, Anthony F. Martone³, Kelly D. Sherbondy³, Ram. M. Narayanan²

¹Radar Systems Lab (RSL), University of Kansas, Lawrence, KS, USA

²Electrical Engineering Department, Pennsylvania State University, University Park, PA, USA

³Sensors and Electron Devices Division, Army Research Laboratory (ARL), Adelphi, MD, USA

Abstract—Cognitive sense-and-avoid (SAA) and sense-and-notch (SAN) emission strategies have recently been experimentally demonstrated as effective ways in which to reduce the interference a spectrum-sharing radar causes to other in-band users. In both cases, however, it has been observed that when the spectral content occupied by the radar changes during the coherent processing interval (CPI) in response to dynamic radio frequency interference (RFI), a nonstationarity in the form of clutter modulation is induced that degrades clutter cancellation. Here the efficacy of joint range/Doppler processing is experimentally assessed for this problem through use of the non-identical multiple pulse compression (NIMPC) method. The additional degrees of freedom provided by this type of approach are shown to compensate for this clutter modulation effect to a significant degree, thus implying a benefit to joint range/Doppler processing in general.

Keywords—*spectrum sharing, cognitive radar, spectrum notching, joint domain filtering, FM noise radar*

I. INTRODUCTION

Increasing spectral congestion and demands for designated radar bands to be opened for other applications is driving an explosion of research into radar spectrum sharing and cognitive radar (e.g. [1-9]). One such perspective is the generation of radar waveforms that seek to mitigate mutual interference between the radar and other in-band users, which is a major focus of recent software-defined radar (SDRadar) development efforts [10]. It has been experimentally shown that different forms of agile waveforms (e.g. [11, 12]) do address this mutual interference issue, though they subsequently necessitate appropriate compensation within the radar receive processing to avoid other forms of performance degradation that this manner of operation otherwise incurs.

Generally classified as forms of sense-and-avoid (SAA) and sense-and-notch (SAN), two recent approaches were developed to accommodate dynamically changing in-band RFI [11, 12]. These approaches rely on fast spectrum sensing (FSS) [13] to assess the spectral environment on a per-pulse basis so as to tailor the next pulsed waveform to minimize mutual interference. In the SAA case [11] this task is accomplished by modifying the center frequency and bandwidth of a linear FM (LFM) chirp so that it occupies the largest available contiguous

bandwidth within the available band. In the SAN case [12] appropriate spectral notches are inserted into a random FM waveform that is unique for each pulse.

These two methods provide different benefits with respect to sensing performance, latency, and computational cost, but they both experience a modulation of the clutter due to their dynamically changing nature. This modulation effect translates into residual clutter that persists after the application of standard cancellation methods and is evidenced by prominent streaks in the resulting range-Doppler response.

This clutter modulation phenomena (caused by pulse-to-pulse waveform adaption to dynamic RFI, and not the RFI itself) can be understood by considering that per-pulse modifications to waveforms during a CPI introduces a coupling between the range and (slow-time) Doppler dimensions. Thus the traditional application of pulse compression and Doppler processing in a sequential, and therefore separate, manner can be viewed as applying insufficient degrees of freedom to the problem. While it has been recently shown that jointly designed pulse compression filters for agile waveform sets [14, 15] and appropriately notched mismatched filtering [16] combined with an ad hoc method for clutter spectrum compensation [17] can do rather well at addressing clutter modulation for a stationary platform, it is expected that their efficacy may be limited for moving platforms when additional angle/Doppler coupling arises.

To that end, here we explore the use of range/Doppler coupled filtering. Specifically, the NIMPC formulation was developed in [18] for use with pulse-agile waveforms that introduce range sidelobe modulation (RSM) of clutter. A variety of these waveform classes have been developed over the last few years (see [19] for an overview). A related approach to this problem was also developed at the same time in [20].

As noted in [17], the clutter modulation involved with dynamically changing spectral notches involves more than clutter RSM, however. It has been observed that moving notches also introduces a modulation of the pulse compression mainlobe, which is why the clutter compensation approach in [17] was proposed. This paper investigates whether the NIMPC method likewise addresses this more severe clutter modulation problem, in so doing determining whether joint

range/Doppler processing methods are generally beneficial in this context.

II. COGNITIVE RADAR OPERATION & WAVEFORMS

Denote the radar waveform transmitted during the m^{th} pulse repetition interval (PRI) of a CPI of M pulses as $s_m(t)$ for $m = 0, 1, \dots, M - 1$. In this context, waveform $s_m(t)$ is arbitrary and can vary on a pulse-to-pulse basis with respect to modulation and/or center frequency, though it is assumed that all M waveforms reside in the same band. The waveforms considered here are, for the SAA case, an LFM chirp with adjustable bandwidth and center frequency, and for the SAN case the pseudo-random optimized (PRO)-FM class of waveforms [21] spectrally notched according to [12].

A timing diagram is shown in Fig. 1 depicting the operation of each waveform type in response to the same dynamic RFI (here considered to be orthogonal frequency division multiplexing (OFDM), though it is not limited to that). The SAN PRO-FM waveforms preserve the 3-dB bandwidth throughout the CPI and place spectral notches to accommodate changing RFI (in green). Some degree of spectral roll-off outside the 3-dB bandwidth (as depicted) depends on the choice of power spectrum template (here it is Gaussian).

Conversely, the SAA LFM waveforms change center frequencies and 3-dB bandwidth to avoid the RFI completely while otherwise occupying the largest bandwidth possible within the overall 3-dB bandwidth (same as PRO-FM case). No roll-off is depicted for the SAA case because LFM provides rather compact spectral content.

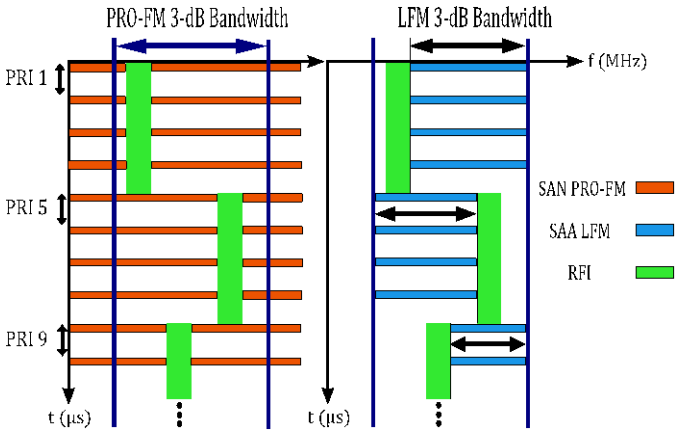


Fig. 1. Timing diagram for SAN PRO-FM and SAA LFM waveforms responding to dynamic RFI on a per-pulse basis

A detrimental consequence of dynamic spectral notching can be observed in Fig. 2, where the autocorrelations (hypothetical responses to a point scatterer) of three different SAN waveforms is shown. Specifically, different spectral notch locations for these waveforms translates into a modulation of the pulse compression mainlobe, which subsequently serves to modulate the clutter. While RSM (also evident in Fig. 2) can be addressed through judicious mismatched filtering [14-16], it is this mainlobe modulation effect that necessitated the devoid clutter capture and filling (DeCCaF) approach in [17]. While not depicted here, SAA LFM experiences the same effect due to variation of bandwidth and center frequency.

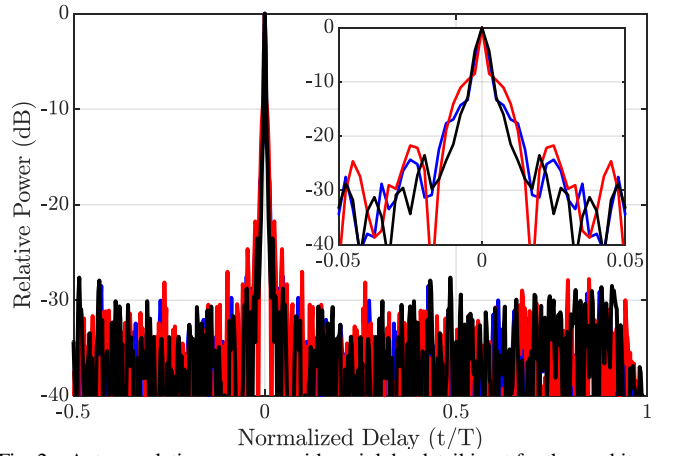


Fig. 2. Autocorrelation response with mainlobe detail inset for three arbitrary SAN waveforms having different spectral notch locations and widths. Note the variation in the mainlobe response.

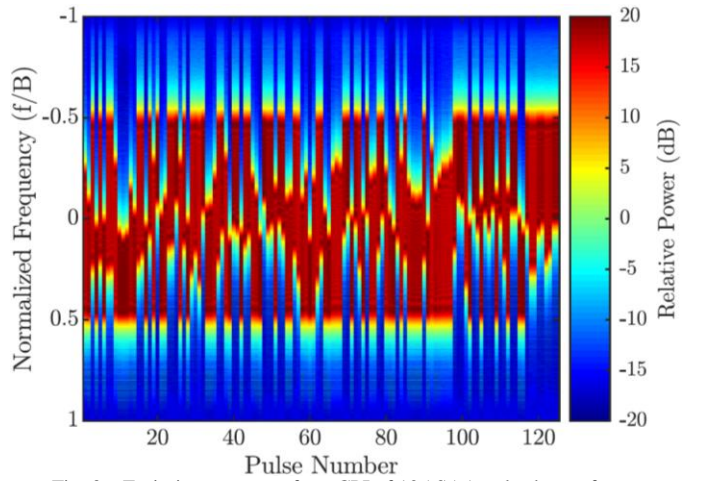


Fig. 3. Emission spectrum for a CPI of 125 SAA pulsed waveforms

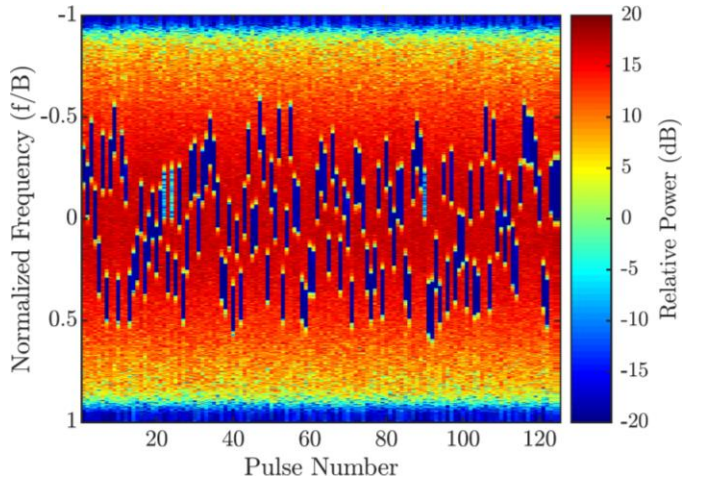


Fig. 4. Emission spectrum for a CPI of 125 SAN pulsed waveforms

Figures 3 and 4 show hardware loopback captures of the emission spectra of SAA and SAN waveforms (though not responding to the same RFI pattern) generated by a Tektronix arbitrary waveform generator (AWG) and subsequently captured on a Rohde & Schwarz real-time spectrum analyzer

(RSA) as described in [12]. In each case a CPI of $M = 125$ pulsed waveforms is produced in response to an emulated RFI source (OFDM with 8 subcarriers and 10 MHz instantaneous bandwidth) that is rapidly moving around the band in a random manner. The overall 3-dB bandwidth possible for both radar emission schemes (demarcated by ± 0.5 in normalized frequency) is 100 MHz and each pulse width is 2 μ s. Thus each SAN waveform has a time-bandwidth product of $BT = 200$, while BT clearly varies for the SAA case. Also, the SAN spectral notches achieve a depth of about 45 dB (relative to the spectrum peak) in this hardware loopback measurement.

The application of receive processing to compensate for clutter modulation requires appropriate discretization of the continuous waveform representation, with the understanding that some aliasing is unavoidable since a time-limited pulse has theoretically infinite bandwidth. Here each waveform is discretized with an “over-sampling” factor of $K = 2$ relative to 3-dB bandwidth. Thus the discretized version of the m^{th} pulse in the CPI is represented as $\mathbf{s}_m = [s_{m,1} \ s_{m,2} \ \dots \ s_{m,N}]^T$, where $N = K(BT)$ is the length of vector \mathbf{s} . The CPI of discretized waveforms can then be collected into the $N \times M$ matrix \mathbf{S} .

III. BRIEF REVIEW OF NIMPC

As developed in [18], the reflected signal for all M pulses in the CPI corresponding to range cell ℓ is represented by the row vector $\mathbf{y}(\ell) = [y_0(\ell) \ y_1(\ell) \ \dots \ y_{M-1}(\ell)]$. The m^{th} element of this vector is defined as

$$y_m(\ell) = \sum_{\theta} [\mathbf{x}_{\theta}^T(\ell) \mathbf{s}_m e^{jm\theta}] + n(\ell), \quad (1)$$

where $\mathbf{x}_{\theta}(\ell) = [x(\ell, \theta) \ x(\ell-1, \theta) \ \dots \ x(\ell-N+1, \theta)]^T$ is a collection of N complex scattering coefficients corresponding to Doppler phase shift θ that convolves with the m^{th} pulsed waveform at delay ℓ , and $n(\ell)$ is complex white noise. These scattering coefficients represent all scatterers in the range profile, comprising both targets of interest and clutter.

Now collect N contiguous fast-time samples of the received signal to construct the matrix

$$\mathbf{Y}(\ell) = \sum_{\theta} [\mathbf{X}_{\theta}(\ell) (\mathbf{S} \odot \mathbf{V}_{\theta})] + \mathbf{N}(\ell), \quad (2)$$

where \mathbf{V}_{θ} is the $N \times M$ matrix formed from the outer product

$$\mathbf{V}_{\theta} = \mathbf{1}_{M \times 1} [1 \ e^{j\theta} \ e^{j2\theta} \ \dots \ e^{j(M-1)\theta}], \quad (3)$$

for $\mathbf{1}_{M \times 1}$ a vector of ones, $\mathbf{N}(\ell)$ is N samples of complex white noise, and \odot denotes the Hadamard product. The $N \times N$ matrix

$$\mathbf{X}_{\theta}(\ell) = \begin{bmatrix} x(\ell, \theta) & x(\ell-1, \theta) & \dots & x(\ell-N+1, \theta) \\ x(\ell+1, \theta) & x(\ell, \theta) & \dots & x(\ell-N+2, \theta) \\ \vdots & \vdots & \ddots & \vdots \\ x(\ell+N-1, \theta) & x(\ell+N-2, \theta) & \dots & x(\ell, \theta) \end{bmatrix} \quad (4)$$

is thus composed of the complex scattering values for the $2N-1$ range cells surrounding $x(\ell, \theta)$. The received signal

matrix in (2) can be rearranged into a single column vector of length NM by performing the vectorization operation as

$$\tilde{\mathbf{y}}(\ell) = \text{vec}\{\mathbf{Y}(\ell)\} = \text{vec}\left\{\sum_{\theta} [\mathbf{X}_{\theta}(\ell) (\mathbf{S} \odot \mathbf{V}_{\theta})] + \mathbf{N}(\ell)\right\}. \quad (5)$$

Therefore a normalized, joint range-Doppler steering vector can be written as [18]

$$\mathbf{w}_{\theta} = \frac{1}{NM} \text{vec}\{\mathbf{S} \odot \mathbf{V}_{\theta}\}, \quad (6)$$

and subsequently employed to estimate complex scatterer $x(\ell, \theta)$ as

$$\hat{x}_{\text{NIMPC}}(\ell, \theta) = \mathbf{w}_{\theta}^H \tilde{\mathbf{y}}(\ell). \quad (7)$$

When the filter in (7) is applied for all range cells ℓ and Doppler phase shift values θ , the result is identical to that obtained from using each waveform’s matched filter followed by standard Doppler processing. However, because the NIMPC framework jointly encompasses the range and (slow-time) Doppler domains, it provides a multiplicative increase in degrees of freedom with which to perform (modulated) clutter cancellation. Consequently, NIMPC addresses the range/Doppler coupling that arises for pulse-agile waveforms.

A simple non-adaptive form of clutter cancellation can be incorporated into NIMPC by constructing the structured range/Doppler covariance matrix [18]

$$\mathbf{R} = \mathbf{P}_{\phi} \mathbf{P}_{\phi}^H + \varepsilon \mathbf{I}, \quad (8)$$

where ε is a diagonal loading factor to make (8) full rank and \mathbf{P}_{ϕ} contains versions of the steering vector that account for the possible delay shifts in each discretized waveform, with values of $\phi = \theta$ associated with clutter Doppler. The NIMPC filter in (6) can thus be modified as

$$\tilde{\mathbf{w}}_{\theta} = \left(\frac{\mu}{NM}\right) \mathbf{R}^{-1} [\text{vec}\{\mathbf{S} \odot \mathbf{V}_{\theta}\}], \quad (9)$$

for μ a scale factor to normalize the filter response. While not addressed here, NIMPC can also be extended to address range-ambiguous clutter (see [18]). Note that we are not suggesting that NIMPC is the solution to this clutter modulation problem but are using it as a general surrogate for all prospective joint range/Doppler approaches since it is relatively straightforward. The incorporation of adaptivity in this context remains a topic of future work.

Finally, a quick examination of computational complexity is warranted. For a CPI of M pulses containing length $N = K(BT)$ discretized waveforms, the joint covariance matrix \mathbf{R} has dimensions $NM \times NM$, which does not include a spatial dimension. For practical CPI size and for waveforms with sufficient BT to necessitate spectral notching, the computation and memory requirements may become prohibitive. For instance, $NM = K(BT)M = 2(200)(125) = 5 \times 10^4$ for Figs. 3 and 4, which would result in an extremely large matrix to invert. Thus while the goal here is to assess the efficacy of joint range/Doppler processing in general, further work is likewise

necessary to realize computationally feasible solutions (e.g. [22]).

IV. EXPERIMENTAL ASSESSMENT OF NIMPC

To evaluate the efficacy of joint range/Doppler processing methods such as NIMPC at compensating for severe clutter modulation effects, the SAA and SAN emissions captured in loopback, with spectra depicted in Figs. 3 and 4, were again generated using the Tektronix AWG and used to illuminate the intersection of 23rd and Iowa Streets in Lawrence, KS from the roof of Nichols Hall on the University of Kansas campus. Moving target indication (MTI) data was captured (again with the RSA) of mostly radially oriented traffic passing through the intersection. As before, both CPIs contain $M = 125$ pulses of SAN and SAA waveforms having $BT = 200$. The CPIs were transmitted back-to-back to capture the same traffic scene for comparison. A picture of the experimental testbed is shown in Fig. 5.



Fig. 5. Photograph of the experimental testbed setup on the roof of Nichols Hall at the University of Kansas in Lawrence, KS.

Note that, while these emission schemes are specifically intended to address dynamic RFI and they were in fact constructed based on the use of FSS RFI sensing [13] and the respective procedures described in [11] and [12], the following measurements do not actually contain RFI. The reason is because we wish to focus on the compensation of clutter modulation alone in a controlled experiment. If this deleterious effect cannot be adequately addressed to enable acceptable sensing performance, then the RFI avoidance/ mitigation aspect becomes a moot point.

As a baseline for comparison, standard matched filter pulse compression and Doppler processing were performed on the received echoes from each emission scheme. Simple projection-based clutter cancellation of zero Doppler was applied since the platform was stationary. The resulting range-Doppler responses for SAA and SAN waveforms are shown in Figs. 6 and 7, respectively.

The streaking induced by severe clutter modulation can be clearly observed in both cases, where the most pronounced streaks at ranges of roughly 1030, 1160, and 1190 meters correspond to large clutter discretets (buildings) near the traffic intersection. Moreover, the streaking is more pronounced in the SAA case (Fig. 6), which is expected since the SAA CPI can

realize greater variation in spectral content on a pulse-to-pulse basis (RFI dependent, of course). That said, SAA is also easier to implement, requires virtually no computational overhead, and therefore the response latency only depends on the speed with which the dynamic RFI location(s) can be determined.

By comparison, the SAN case (Fig. 7) has somewhat more diffused streaking because the overall 3-dB bandwidth is preserved (see Fig. 1) and thus the amount of mainlobe modulation (like in Fig. 2) is less severe. For practical applications this result is still unacceptable, however.

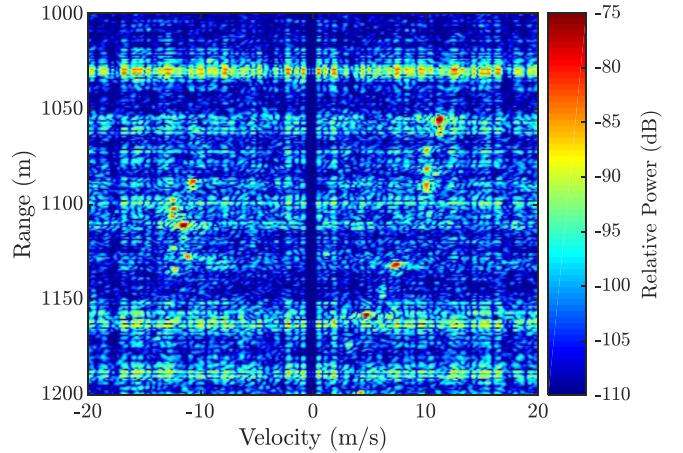


Fig. 6. Measured range-Doppler response for SAA waveforms from [11] using standard pulse compression and Doppler processing.

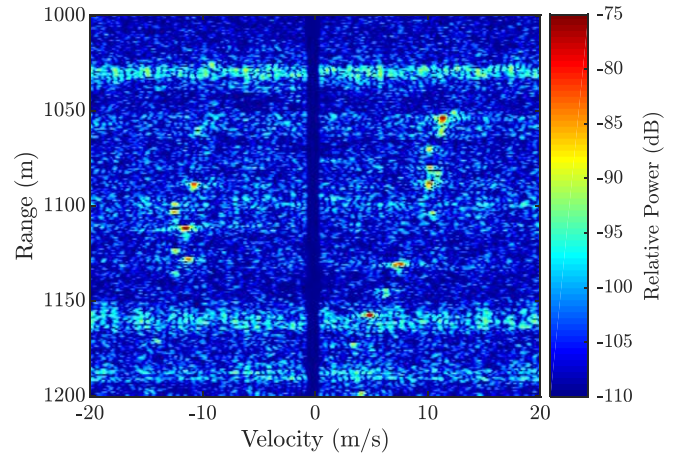


Fig. 7. Measured range-Doppler response for SAN waveforms from [12] using standard pulse compression and Doppler processing

Another useful point of comparison is to consider the combination of least-squares (notched) mismatched filtering (LS-MMF) [16] and ad hoc clutter filling via DeCCaF [17]. The former suppresses range sidelobes to combat RSM effects while the latter seeks to homogenize the clutter spectrum over the CPI as a means to mitigate mainlobe modulation. These results are shown in Figs. 8 and 9 for SAA and SAN waveforms, respectively. Compared to standard processing in Figs. 6 and 7, both sets reveal noticeable reduction in clutter modulation effects, with the remaining streaks in the SAN case only barely discernible. The more modest improvement for the SAA case is again due to the greater variation in spectral

content over the CPI, making these effects more difficult to compensate.

As noted in [17], the DeCCaF approach is an ad hoc solution that, while certainly providing some compensation benefit (with an almost negligible computational cost), it does pose some limitations. These limits include 1) the need for available clutter spectrum from other pulses from which to “borrow” and 2) the lack of statistical independence when reusing borrowed clutter. The former may be particularly restrictive for the SAA case because there is simply less spectrum available in other pulses. Consequently, while the LS-MMF/DeCCaF combination has clear practical benefits, it is by no means a panacea.

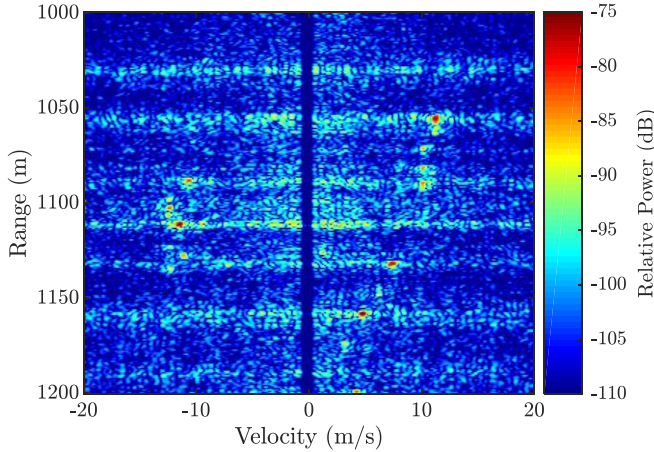


Fig. 8. Measured range-Doppler response for SAA waveforms from [11] using LS-MMF [16] and DeCCaF clutter filling [17]

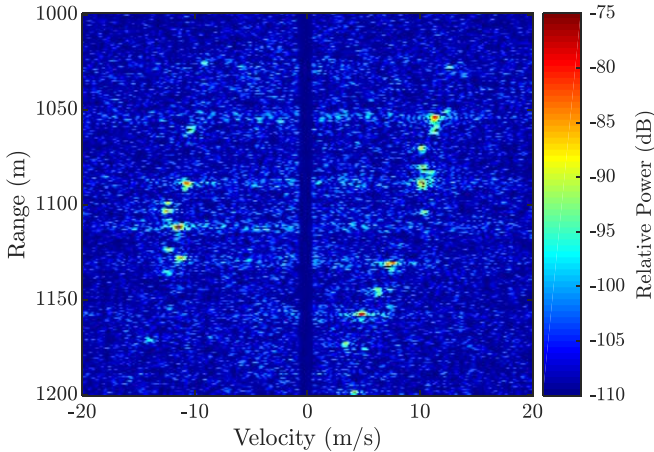


Fig. 9. Measured range-Doppler response for SAN waveforms from [12] using LS-MMF [16] and DeCCaF clutter filling [17]

Finally, joint range/Doppler processing via NIMPC from (9) is considered for the two emission schemes. Using the parlance of [18], $Q = 3$ “clutter notches” centered on zero Doppler were used (not to be confused with spectral notches). It was found that further increasing Q did not provide any observable benefit in terms of clutter cancellation.

Figures 10 and 11 illustrate the NIMPC results for these data sets, where it is observed that the residual clutter modulation streaks are further reduced for the SAA case (compared to Fig. 8). For the SAN case, these streaks are at

essentially the same level as in the LS-MMF/DeCCaF result, but the remaining speckle elsewhere has been reduced. Thus, from a qualitative standpoint, we can say that joint range/Doppler processing does indeed provide further clutter modulation compensation capability. Even further reduction may be possible if appropriate adaptivity can be incorporated.

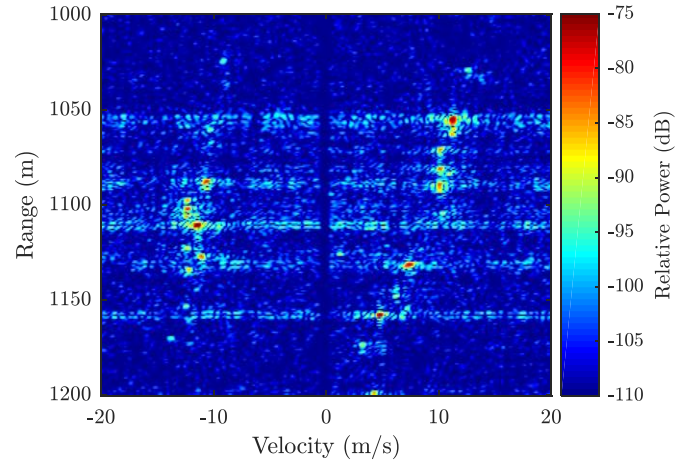


Fig. 10. Measured range-Doppler response for SAA waveforms from [11] using NIMPC from (9) [18]

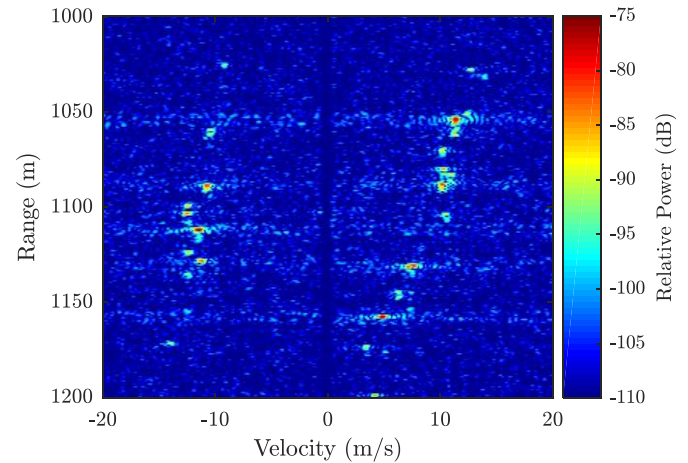


Fig. 11. Measured range-Doppler response for SAN waveforms from [12] using NIMPC from (9) [18]

It is interesting to compare the 3 processing methods for each emission scheme for a Doppler slice at a single range bin. Figures 12 and 13 illustrate this comparison for SAA and SAN, respectively, at a range of 1055 m where a large moving target resides. For both data sets joint range/Doppler processing as exemplified by NIMPC exhibits the lowest background response (residual clutter + noise) and very little SNR loss relative to standard matched filter (MF) processing (from Figs. 6 and 7). The MMF+DeCCaF results have a mismatch loss of 1.5 and 3.0 dB for the SAA and SAN emissions, respectively, with the former also experiencing some increase in the background floor at this particular range (though comparing Figs. 6 and 8 show this effect to be an isolated incident). It is also interesting to note that the moving target response is 2.6 dB higher for the SAA case, which may be due to extreme spectral containment of the LFM waveform

(relative to more gradual roll-off for random FM waveforms) experiencing less bandlimiting loss in the RSA capture.

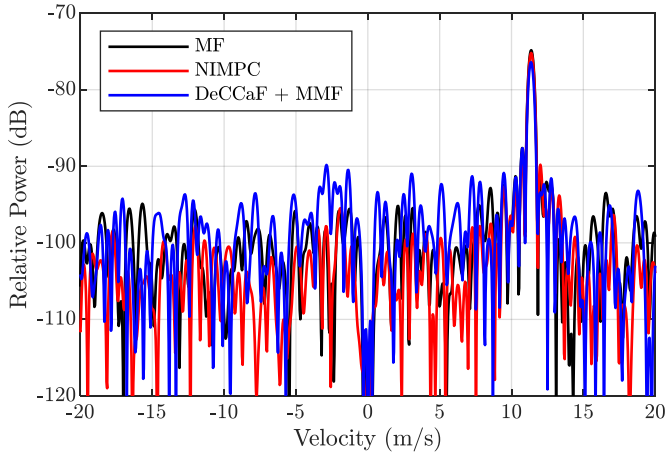


Fig. 12. Measured Doppler slice at a range of 1055 m for SAA waveforms using standard processing, NIMPC, and MMF+DeCCaF

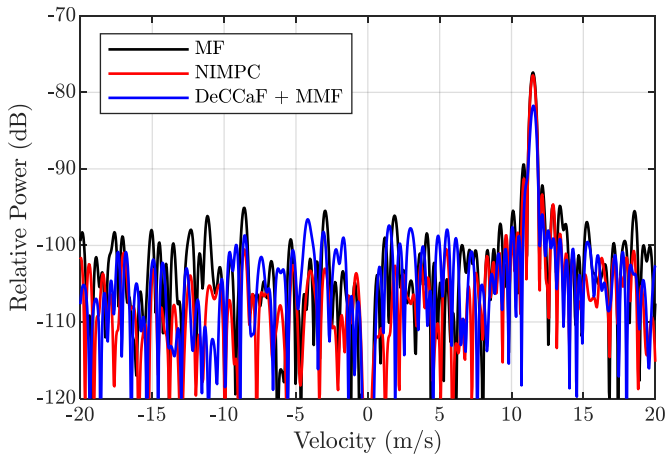


Fig. 13. Measured Doppler slice at a range of 1055 m for SAN waveforms using standard processing, NIMPC, and MMF+DeCCaF

CONCLUSIONS

The NIMPC method has been used to experimentally demonstrate the efficacy of joint range-Doppler processing in general as a viable means with which to compensate for the severe clutter modulation caused by waveforms changing during the CPI to contend with dynamic RFI. Moreover, this joint approach has been found to be superior to the recent ad hoc combination of LS (notched) mismatched filtering and clutter borrowing/filling by DeCCaF. The reason for this superiority is because dynamically changing the waveforms to address dynamic RFI introduces an inherent coupling between range and (slow-time) Doppler. Of course, as is generally the case, coupled forms of processing incur a higher computational cost. It remains to be seen how adaptivity can be properly integrated into formulations of this type. The incorporation of spatial degrees of freedom to address angle/Doppler coupling induced by platform motion likewise remains a topic of ongoing investigation.

REFERENCES

- [1] H. Griffiths, L. Cohen, S. Watts, E. Mokole, C. Baker, M. Wicks, S. Blunt, "Radar spectrum engineering and management: technical and regulatory Issues," *Proc. IEEE*, vol. 103, no. 1, pp. 85-102, Jan. 2015.
- [2] M. Labib, V. Marojevic, A.F. Martone, J.H. Reed, A.I. Zaghoul, "Coexistence between communications and radar systems – a survey," *URSI Radio Science Bulletin*, vol. 2017, no. 362, pp. 74-82, Sept. 2017.
- [3] J.M. Peha, "Sharing spectrum through spectrum policy reform and cognitive radio," *Proc. IEEE*, vol. 97, no. 4, pp. 708-719, Apr. 2009.
- [4] P. Stinco, M.S. Greco, F. Gini, "Spectrum sensing and sharing for cognitive radars," *IET Radar, Sonar & Navigation*, vol. 10, no. 3, pp. 595-602, Feb. 2016.
- [5] A. Farina, A. DeMaio, S. Haykin, *The Impact of Cognition on Radar Technology*, IET, 2017.
- [6] S.D. Blunt, E.S. Perrins, *Radar & Communication Spectrum Sharing*, IET, 2018.
- [7] L. Zheng, M. Lops, Y.C. Eldar, X. Wang, "Radar and communication coexistence: an overview," *IEEE Signal Processing Magazine*, vol. 36, no. 5, pp. 85-99, Sept. 2019.
- [8] K.V. Mishra, M.R. Bhavani Shankar, V. Koivunen, B. Ottersten, S.A. Vorobyov, "Toward millimeter-wave joint radar communications," *IEEE Signal Processing Mag.*, vol. 36, no. 5, pp. 100-114, Sept. 2019.
- [9] A. Hassanien, M.G. Amin, E. Aboutanios, B. Himed, "Dual-function radar communication systems," *IEEE Signal Processing Mag.*, vol. 36, no. 5, pp. 115-126, Sept. 2019.
- [10] A.F. Martone, K.D. Sherbondy, J.A. Kovarskiy, B.H. Kirk, C.E. Thornton, et al., "Metacognition for radar coexistence" *IEEE Intl. Radar Conf.*, Washington, D.C., Apr. 2020.
- [11] B.H. Kirk, R.M. Narayanan, K.A. Gallagher, A.F. Martone, K.D. Sherbondy, "Avoidance of time-varying radio frequency interference with software-defined cognitive radar," *IEEE Trans. Aerospace & Electronic Systems*, vol. 55, no. 3, pp. 1090-1107, June 2019.
- [12] B. Ravenscroft, J.W. Owen, J. Jakabosky, S.D. Blunt, A.F. Martone, K.D. Sherbondy, "Experimental demonstration and analysis of cognitive spectrum sensing and notching for radar," *IET Radar, Sonar & Navigation*, vol.12, no.12, pp. 1466-1475, Dec. 2018.
- [13] A.F. Martone, K.I. Ranney, K. Sherbondy, K.A. Gallagher, S.D. Blunt, "Spectrum allocation for noncooperative radar coexistence," *IEEE Trans. Aerospace & Electronic Systems*, vol. 54, no. 1, pp. 90-105, Feb. 2018.
- [14] A.C. O'Connor, J.M. Kantor, J. Jakabosky, "Filters that mitigate waveform modulation of radar clutter," *IET Radar, Sonar & Navigation*, vol. 11, no. 8, pp. 1188-1195, July 2017.
- [15] C. Sahin, J.G. Metcalf, S.D. Blunt, "Filter design to address range sidelobe modulation in transmit-encoded radar-embedded communications," *IEEE Radar Conf.*, Seattle, WA, May 2017.
- [16] B. Ravenscroft, J.W. Owen, S.D. Blunt, A. F. Martone, K.D. Sherbondy, "Optimal mismatched filtering to address clutter spread from intra-CPI variation of spectral notches," *IEEE Radar Conf.*, Boston, MA, Apr. 2019.
- [17] J.W. Owen, B. Ravenscroft, S.D. Blunt, "Devoid clutter capture and filling (DeCCaF) to compensate for intra-CPI spectral notch variation," *Intl. Radar Conf.*, Toulon, France, Sept. 2019.
- [18] T. Higgins, K. Gerlach, A.K. Shackelford, S.D. Blunt, "Non-identical multiple pulse compression and clutter cancellation," *IEEE Radar Conf.*, Kansas City, MO, May 2011.
- [19] S.D. Blunt, J.K. Jakabosky, C.A. Mohr, P.M. McCormick, J.W. Owen, et al, "Principles and applications of random FM radar waveform design," to appear in *IEEE AES Systems Mag.*
- [20] D.P. Scholnik, "Range-ambiguous clutter suppression with pulse-diverse waveforms," *IEEE Radar Conf.*, Kansas City, MO, May 2011.
- [21] J. Jakabosky, S.D. Blunt, B. Himed, "Spectral-shape optimized FM noise radar for pulse agility," *IEEE Radar Conf.*, Philadelphia, PA, May 2016.
- [22] C. Sahin, J.G. Metcalf, B. Himed, "Reduced complexity maximum SINR receiver processing for transmit-encoded radar-embedded communications," *IEEE Radar Conf.*, Oklahoma City, OK, Apr. 2018.